

CONTRAST-ENHANCED FLOW IMAGING WITH PHASE-CODED PULSE SEQUENCES

W. Wilkening¹, B. Brendel¹, V. Uhlendorff², H. Ermert¹

¹Institute of High Frequency Engineering, Faculty of Electrical Engineering,
Ruhr-Universitaet Bochum, Germany

²Research Laboratories of Schering AG, Berlin, Germany

Abstract – The effect of nonlinear scattering from microbubbles is commonly used for contrast specific imaging. Linear scattering from microbubbles is not contrast specific, yet it contributes more to the echo signal. To optimize flow imaging with contrast agents, it is desirable to exploit linear scattering and nonlinear scattering to improve sensitivity without sacrificing specificity. This can be achieved by incorporating the amplitude and phase dependencies of the fundamental and harmonic spectral components in the Doppler processing. The separability of the aforementioned components is achieved by phase- (or amplitude-) coding of the transmit pulses.

INTRODUCTION

The measurement of blood flow velocities is a challenging task, since strong echoes from out-of-plane structures and reverberation superimpose the echoes from actually flowing scatterers. Wall filters solve this problem satisfactorily for high flow velocities. With the introduction of nonlinear imaging techniques for contrast agents evaluating the 2nd harmonic signal component seemed to be promising for imaging slow flow velocities [1, 2]. The fundamental signal component, however, contains more energy. Thus, it is desirable to include both signal components in the flow estimation [3]. This can be done by an independent evaluation of both components. We have worked on a strategy that combines both components (and echoes from stationary scatterers) in one estimator, thus taking into account the common origin of both signals.

Standard pulsed Doppler systems transmit a train of N pulses along the same beam line. Each firing starts at $t=0$, where t denotes the “fast time”. The time interval between subsequent pulse is given by $T_{\text{prt}} = 1/f_{\text{prf}}$, where f_{prf} is referred to as the pulse repetition frequency and defines the sampling rate

along the “slow time”. The transmit pulses can be written as

$$s_i(t) = \alpha_i \cdot g(t) \cdot \cos(\omega_0 t + \varphi_i), \quad i = 1 \dots N, \quad (1)$$

$$\alpha_i, \varphi_i \in \mathbb{R},$$

where $g(t)$ is the envelope, ω_0 the carrier frequency, and α_i, φ_i consider amplitude and phase coding, respectively. In the following, we will focus on a sequence without amplitude-coding and with phase-coding, where 4 phases are repeated several times:

$$\varphi_i = [\varphi_1, \varphi_2 \dots \varphi_N] = [\varphi_1, \varphi_2, \varphi_3, \varphi_4, \varphi_1 \dots \varphi_4], \quad (2)$$

$$N = 4k, k \in \mathbb{N}, \quad \alpha_i = \alpha$$

In response to the transmit signals, echoes are received and quadrature demodulated into complex baseband signals $e_{B_i}(t)$. The mixing frequency and filters are chosen to include fundamental and 2nd harmonic spectral components. The baseband signal is commonly evaluated at constant depth $t = 2z/c_0$ in slow time-direction denoted by i , where c_0 is the speed of sound and $t_s = (i-1)T_{\text{prt}}$. Assuming the most basic model for linear scatterers moving at the velocity v with respect to the beam direction, the baseband signal is given by:

$$e_{B_i}(t) \Big|_{t=\text{const}=2z_0/c_0} = e_{B_i, z_0} = \beta e^{j\omega_D t_s} e^{j\varphi_i}, \quad (3)$$

$$\beta \in \mathbb{C}, \quad \beta \propto \alpha, \quad \omega_D = 2\pi \frac{2v}{\lambda} = 2 \frac{v\omega_0}{c_0}$$

We expand the model to account for stationary scatterers, described by the complex constant α and a nonlinear moving scatterer that is described by a fundamental term (linear term) and a 2nd harmonic term (quadratic term). The “DC” (broadband) component that is created by the quadratic term will be neglected.

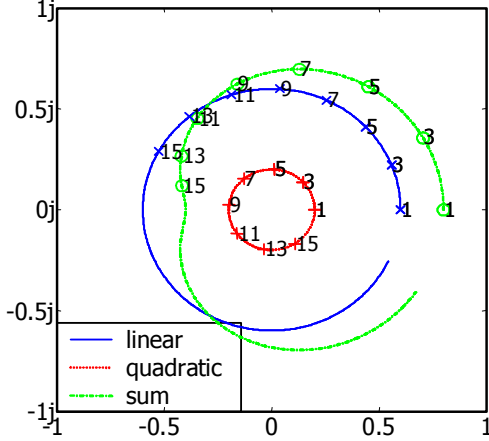


Fig. 1: Plot of \tilde{e}_{Bi,z_0} ($o=0$) without phase-coding.

$$e_{Bi,z_0} = \beta e^{j\omega_D t_s} e^{j\phi_i} + \gamma e^{2j\omega_D t_s} e^{2j\phi_i} + o e^{j\phi_i}, \quad (4)$$

$$\beta, \gamma, o \in \mathbb{C}, \quad \beta \propto \alpha, \quad \gamma \propto \alpha^2$$

Note that β and γ being complex allow the fundamental and the 2nd harmonic component to have independent initial phase angles. Equation (4) can be rewritten as

$$e_{Bi,z_0} = e^{j\phi_i} (\beta e^{j\omega_D t_s} + \gamma e^{2j\omega_D t_s} e^{j\phi_i} + o) = e^{j\phi_i} \tilde{e}_{Bi,z_0} \quad (5)$$

As can be seen from (5), the phase coding cannot be factored out of the quadratic term, and the quadratic term has twice the flow-related phase shift as compared to the linear term.

The following figures exemplify the influences of flow and phase-coding on \tilde{e}_{Bi,z_0} in absence of a linear, stationary scatterer ($o=0$). Fig. 1 shows \tilde{e}_{Bi,z_0} in the case of a slowly moving nonlinear scatterer without phase-coding: $f_{\text{prf}} = 1 \text{ kHz}$, $\omega_D = 2\pi \cdot 30 \text{ Hz}$, $\beta = 0.6$, $\gamma = 0.2$, $\phi_i = 0$, $N = 32$.

The linear term shows an increase in phase angle according to the Doppler frequency. The quadratic term expectedly exhibits twice the increase in phase angle. The superposition of both terms yields a deformed circle with uneven spacing of data points along the curve, indicating that standard algorithms may not measure the velocity correctly.

Next, phase-coding with a phase increment of $-\pi/2$ is applied to the transmit pulses. The curve for the linear term in Fig. 2 remains unchanged, since the

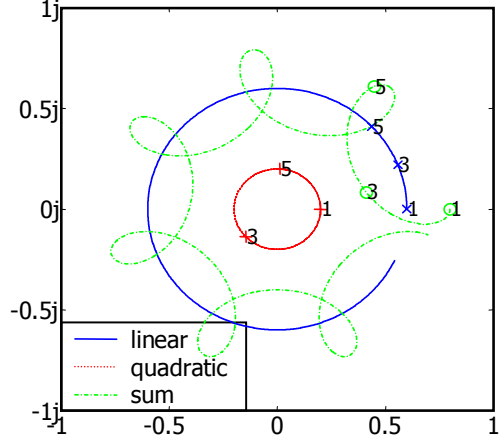


Fig. 2: Plot of \tilde{e}_{Bi,z_0} ($o=0$) with phase-coding.

phase-coding is compensated in \tilde{e}_{Bi,z_0} . The quadratic term reflects the phase-coding (clockwise) and the flow (counter clockwise). Because of the flow, the 5th measurement does not complete the first circle ($-4\pi/2 + 2\omega_D 4T_{\text{prt}} = -2\pi + 0.48\pi$. Note that the orientation of the curve is clockwise, since it is dominated by the phase-coding.). It is obvious from Fig. 2 that the phase-coding improves the separation between signals from linear and nonlinear scatterers, respectively.

FLOW VELOCITY ESTIMATION

To correctly measure the flow velocity and to discriminate nonlinear from linear scattering it is necessary to estimate all parameters in (5). Due to the non-linearity of the equation and the dimension of the optimization problem (4 unknown variables), no simple least-square estimator can be found. Given that an initial estimate for ω_D exists, (5) turns into a linear equation with respect to β , γ and o . We denote:

$$\tilde{e}_{Bi,z_0} = \beta \underbrace{e^{j\omega_D (i-1)T_{\text{prt}}}}_{x_i} + \gamma \underbrace{e^{2j\omega_D (i-1)T_{\text{prt}}}}_{y_i} e^{j\phi_i} + o \quad (6)$$

To find optimal values for β , γ and o , the error

$$\begin{aligned} & \left| \tilde{e}_{Bi,z_0} - \beta x_i - \gamma y_i - o \right|^2 = \\ & \left[\operatorname{Re} \left(\tilde{e}_{Bi,z_0} - \beta x_i - \gamma y_i - o \right) \right]^2 \\ & + \left[\operatorname{Im} \left(\tilde{e}_{Bi,z_0} - \beta x_i - \gamma y_i - o \right) \right]^2 \end{aligned} \quad (7)$$

has to be minimized. The unknown variables are chosen so that the partial derivatives of (7) are zero.

Thus, the solution of a system of 6 linear equations yields the real and imaginary parts of aforementioned parameters. To determine all parameters, ω_D is optimized based on (7), where β , γ and o are estimated anew in every optimization step. An initial estimate for ω_D can easily be determined by standard Doppler processing. For this purpose, the 2nd harmonic is filtered out in the fast time domain to minimize the error that is due to non-linear scattering.

The estimated parameters represent the flow velocity of moving scatterers and the amplitudes and phase angles for the fundamental and 2nd harmonic spectral component coming from these scatterers. Additionally, stationary scatterers are considered.

IN VITRO MEASUREMENTS

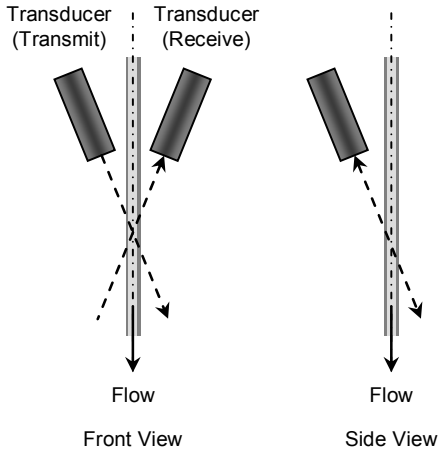


Fig. 3: Schematic drawing of the experimental setup.

The applicability of the model and flow estimation algorithm was tested by means of in vitro measurements. A tube with an outer diameter of 8 mm and an inner diameter of 6 mm was placed into a water tank.

Two broadband 15 MHz transducers (Panametrics V319) with calibrated frequency responses were used to transmit and receive ultrasound, respectively. The transducers were fixed so that the beam lines crossed confocally inside the tube enclosing an angle of about 45°. The angle between the sound propagation directions and the direction of the flow also measures 45°. The geometry is shown in Fig. 3.

Transmit pulses were generated using an arbitrary function generator (LeCroy LW 410A) connected to an ENI A300 amplifier. RF data were collected with a LeCroy 9350AL oscilloscope after pre-amplification and 20 MHz lowpass filtering. The setup was computer controlled to allow the exact acquisition of multiple repetitions of specified sequences.

Several data sets were acquired at different flow velocities ranging from -9 cm/s to 15 cm/s, where positive velocities point away from the transducers. The asymmetry of the velocity range is mostly due to the fact that the radiation force accelerates the microbubbles away from the transmitting transducer. Instead of a pump, gravity was used to produce the desired flow velocities. The microbubbles with a diameter of a few microns were air-filled and encapsulated in a polymer shell. The shell is known to break during the first insonation of a pulse sequence.

Sequences of 32 broadband pulses with a center frequency of 3 MHz were transmitted at a pulse repetition frequency of $1/120\mu\text{s}=8.3\text{ kHz}$. Due to the low concentration of microbubbles and the limited lifespan, only the first 10-20 echoes turned out to be useful.

RESULTS

In the case of strong nonlinear response ($|\beta|/|\gamma| < 2$), the model given in (4) reaches its limits of applicability, although the typical features presented in Fig. 2 can be observed under such conditions, see Fig. 4. In this example, $|\beta|/|\gamma| \approx 1.8$, the flow velocity is 10.5 cm/s. There is also a phase shift of 109° between the fundamental and 2nd harmonic signal components. The comparison of the measured data and the model fitted to the data reveals a discrepancy concerning the phase angles, indicating that the model is too simple to correctly predict the response of microbubble to different carrier phases.

The flow estimations of the estimator described above were compared to those obtained from a linear

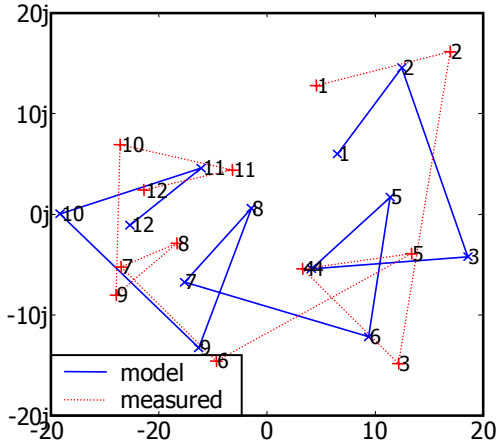


Fig. 4: Measurements of \tilde{e}_{Bi, z_0} and model fitted to the measured data.

model, i.e. (5) without the term $\gamma e^{2j\omega_b t/s} e^{j\phi_i}$. In the case of a broad receive bandwidth, the latter estimator overestimated the flow velocities significantly. A narrow receive filter (1 MHz bandwidth centered around 3 MHz) improved the results of the linear estimator and corrected the overestimation of flow velocities. An analysis of the standard deviation, however, showed an improvement in the signal-to-noise ratio of about 6 dB for the nonlinear model.

CONCLUSIONS

The proposed estimator is an attempt to fully exploit the properties of microbubbles for flow imaging. The results show that the proposed nonlinear estimator outperforms the linear estimator. Moreover, the nonlinear estimator determines the amplitudes for the fundamental and 2nd harmonic signal components so that linear scattering can be discriminated from nonlinear scattering.

Future work will include measurements for varieties of pressure amplitudes and microbubbles concentrations. It might also be necessary to extend the model to two nonlinear, moving media to better account for motion artifacts and tissue harmonics.

ACKNOWLEDGEMENT

The work was carried out by the Ruhr Center of Excellence for Medical Engineering (KMR Bochum), BMBF (Federal Ministry of Education and Research, Germany) grants 13N8017 and 13N8079.

REFERENCES

- [1] D. H. Simpson, C. T. Chin, P. N. Burns, "Pulse Inversion Doppler: A New Method for Detecting Nonlinear Echoes from Microbubble Contrast Agents", IEEE Trans. on UFFC, vol. 46, no. 2, March 1999.
- [2] US Patent: US6155981: Diagnostic ultrasonic imaging system and method for discriminating nonlinearities; beantragt: November 1998; H. Ermert, J. Lazenby, M. Krueger, C. Chapman, W. Wilkening.
- [3] M. Bruce, M. Averkiou, J. Powers, K. Beach, "Vascular and Perfusion Imaging with Ultrasound Contrast Agents", Proceedings of "The Ninth European Symposium on Ultrasound Contrast Imaging", Rotterdam, The Netherlands, January 2004.